Strain relaxation and surface migration effects in InGaAlAs and InGaAsP selective-area-grown ridge waveguides

A. A. Sirenko[a)]
Department of Physics, New Jersey Institute of Technology, Newark, New Jersey 07102

A. Kazimirov
Cornell High Energy Synchrotron Source (CHESS), Cornell University, Ithaca, New York 14853

A. Ougazzaden
Laboratoire Matériaux Optique, Photonique et Systèmes, Université de Metz/Supelec, 57070 Metz, France

S. M. O'Malley
Department of Physics, New Jersey Institute of Technology, Newark, New Jersey 07102

D. H. Bilderback
Cornell High Energy Synchrotron Source (CHESS), Cornell University, Ithaca, New York 14853

Z.-H. Cai, B. Lai, and R. Huang
Advanced Photon Source, 9700 S. Cass Avenue, Argonne, Illinois 60439

V. K. Gupta and M. Chien
TriQuint Optoelectronics, Breinigsville, Pennsylvania 18031

S. N. G. Chu
Multiplex Inc., South Plainfield, New Jersey 07080

(Received 21 November 2005; accepted 23 January 2006; published online 23 February 2006)

Surface migration of the group-III precursors and strain relaxation at the ridge sidewalls are compared for 2.5 μm wide waveguides based on InGaAsP and InGaAlAs multiple-quantum-well (MQW) structures. The cross-sectional thickness and strain variations have been measured using synchrotron radiation-based x-ray diffraction with an angular resolution of 2 arc s and a beam size of (0.24×0.35) μm^2. Indium-rich overgrowth has been observed for the InGaAsP-based waveguides, while InGaAlAs-based waveguides demonstrate thickness uniformity of the MQW active region with a strain relief of 0.4%/μm at the sidewalls. © *2006 American Institute of Physics*. [DOI: 10.1063/1.2177634]

Optoelectronics is progressing from the hybrid integration of individual device chips to high-density monolithic integration of multifunctional optoelectronic structures. Utilization of the strain relaxation on the sidewalls of nanostructures is believed to be the key to the monolithic integration of dissimilar materials with complementary optical and electronic properties.[1] To support this trend, a better understanding of the fundamental growth mechanisms on the nanoscale level, control of the sidewall quality, and a development of the adequate materials characterization tools, such as synchrotron radiation high-resolution x-ray diffraction (HRXRD) are required. In this letter we will demonstrate that the nondestructive HRXRD technique can provide accurate analytical information about the thickness and composite strain variation across the ridge waveguides with submicron spatial resolution. We utilized this technique for comparison between micron-wide InGaAlAs- and InGaAsP-based waveguides produced in a one-growth-step by metal organic vapor-phase epitaxy (MOVPE) in the regime of selective-area growth (SAG).[2–4]

Two samples with conventional 1.3 μm light-emitting laser structures, one with InGaAsP- and another with InGaAlAs-based MQWs, were grown using identical SAG masks on InP (001) substrates.[5] The 600 μm long waveguides with a nominal ridge width of 2.5 μm were formed between the pairs of SiO_2 masks with the width of 14 μm. The active region in both samples consisted of the MQWs with $N=9$ periods and two 50 nm thick separate confinement layers (SCL). Parameters of the investigated samples in the open part of the wafers (far from the oxide mask) are listed in Table I, where strain is expressed in terms of the perpendicular d-spacing mismatch ($S=\Delta d/d$) with respect to the InP substrate.

HRXRD characterization was carried out at the APS 2ID-D microscope beamline equipped with a phase zone plate.[6] High angular resolution was provided by a perfect Si(004) crystal analyzer with an acceptance range within the "intrinsic" rocking curve width of 2.17 arc s.[5] The measure-

TABLE I. Parameters of the investigated samples.

	$In_xGa_yAl_{1-x-y}As$		$In_xGa_{1-x}As_yP_{1-y}$	
	Open wafer	Ridge	Open wafer	Ridge
Well width (nm)	5.0	6.5	7.0	8.9
Barrier width (nm)	10.3	12.9	9.9	13.2
Global strain (%)	0.22	1.15	0.49	0.75
Well composition	$x=0.65$		$x=0.85$	
	$y=0.19$		$y=0.57$	
Barrier composition	$x=0.48$		$x=0.87$	
	$y=0.19$		$y=0.29$	

[a)]Electronic mail: sirenko@njit.edu

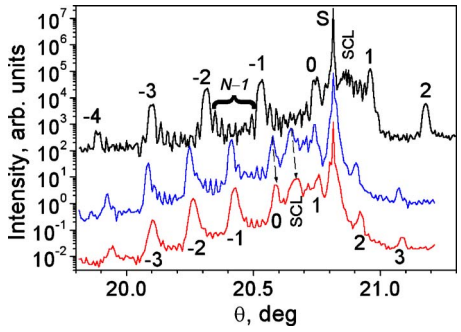

FIG. 1. (Color online) X-ray diffraction from the InGaAlAs-based MQW in the open part of the wafer (upper curve), from the center (middle curve), and from the edge of the same 2.5 μm wide SAG ridge (bottom curve). The MQW satellite peaks are marked according to their order $(-4,-3,-2,\ldots)$ and the diffraction curves are vertically offset for clarity. The substrate InP 004 peaks at $\theta=20.81$ deg with FWHM=7.6 arc s are marked with *S*. Arrows show the shift of the MQW global-strain peak ("0") and separate confinement layer (SCL) peak that indicates the strain change across the ridge.

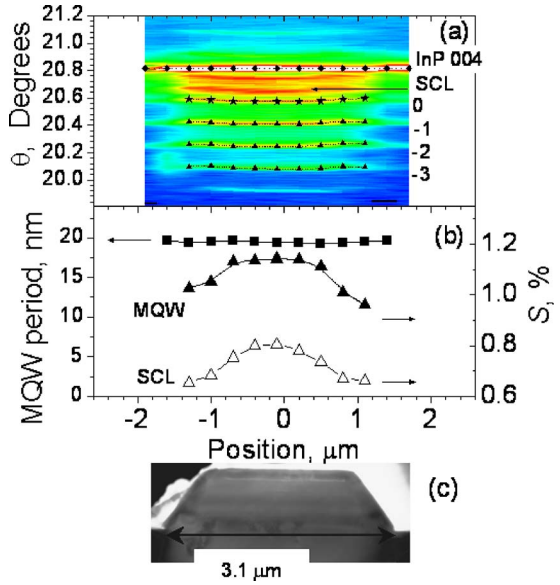

FIG. 2. (Color online) Cross-section analysis of the InGaAlAs-based MQW SAG structure. (a) Diffraction intensity map measured for different positions of the x-ray beam across the ridge. Position of the MQW satellite peaks is marked with triangles, the "0" peak is marked with stars, and the InP 004 substrate peak position is marked with diamonds. (b) MQW period (solid squares) and variation of the global strain (solid triangles) across the ridge. Strain variation in SCL layers is shown with open triangles. (c) Low-magnification TEM image with the shadow of uniform MQWs across the ridge.

ments were performed at an energy of 11.89 KeV. Both the measured FWHM of the InP(004) substrate peak (7.6 arc s) and the observed $(N-1)$ Kiessig fringes between the superlattice peaks demonstrate excellent angular resolution of our setup. By performing $\theta-2\theta$ scans, where θ and 2θ denote rotation angles of the sample and the detector arm, respectively, the diffraction profiles (Fig. 1) were measured over a wide range of $\Delta\theta\approx 2$ deg. The size of the focused x-ray beam was 0.35 μm in the diffraction plane and 0.24 μm in the direction normal to the diffraction plane. The position of the microbeam was controlled with 50 nm precision by monitoring Ga-*K* and As-*K* fluorescence from the ridge structures. The bright-field TEM micrographs were taken at a [002] diffraction condition using a Philips TM420 transmission electron microscope operated at 120 KV.

Figure 1 shows diffraction profiles measured in the center of the SAG ridges for InGaAlAs-based waveguides and in the open part of the wafer. The relative position of the zero-order peak with respect to the InP substrate peak gives the global strain of the MQW structure: $S=(W_W\cdot S_W+W_B\cdot S_B)/(W_W+W_B)$, where $W_{W(B)}$ and $S_{W(B)}$ are the thickness and strain of the well(barrier), respectively. The separation of the superlattice peaks determines the MQW period $T=W_W+W_B$. The HRXRD spectra measured in the center of the ridge waveguides show an increase of both the MQW period and global strain compared to that in the open part of the wafer. Similar to the procedure described in Ref. 5, we were able to determine the thickness of the well and barrier layers (see Table I) through the use of the commercial RADS-Mercury BEDE software.[7]

The vertical and lateral vapor-phase diffusion processes (VVP and LVP, respectively) and the surface migration of the metallorganic precursors are the three main mechanisms with different characteristic lengths that result in the thickness enhancement and compositional changes in the SAG regime.[2–4] Previous microbeam HRXRD studies of SAG structures with different ridge widths and surrounding oxide masks[8–11] have provided significant contributions to the development of the gas-phase diffusion models for SAG processes and allowed accurate calculations of the VVP and LVP effects with characteristic diffusion lengths in the range of 25 to 200 μm.[12–14] In contrast, extensive investigation of the surface migration of the reacting metallorganic species within a typical diffusion length of a few microns has been carried out so far with imaging techniques only[2,3,13,14] and limited information is available on the strain and composition variation caused by this effect.[15,16] The long-range diffusion processes alone cannot properly describe the specifics of the micron-wide ridge formation in the SAG regime. Below, we present experimental results for the surface migration effects and strain relaxation at the ridge sidewalls obtained with our HRXRD setup.

Cross-section measurements for InGaAlAs-based SAG structure are shown in Fig. 2. Within the error bars of $\delta T=\pm 0.1$ nm, the period of MQW ($T=19.4$ nm) is constant across the ridge. This HRXRD result is additionally confirmed by the measured As-*K* fluorescence profile and TEM cross-sectional image [Fig. 2(c)]. Thickness uniformity across the ridge indicates that the surface migration of the group-III precursors during growth is strong enough to remove any excess of the precursor species from the 111-plane terminated sidewalls and to deliver them to the much faster-growing 001 top plane. Strain in the MQW part of the structure (that was measured with accuracy of $\delta S=\pm 0.02\%$) decreases by 0.20% when the x-ray beam is scanned from the center part ($S=1.15\%$) to the edge ($S=0.95\%$) of the ridge. Similar change of the strain was observed for the SCL part of the same ridge structure [Fig. 2(b)]. Since a constant thickness in MOVPE-grown multilayer structures usually indicates a uniform composition for each layer,[17] this effect of the strain decrease should be related to the relaxation of elastic strain at the waveguide sidewalls. The freestanding surface of the ridge terminated by the 111 plane cannot support the same elastic strain as that in the center of the ridge ($S=1.15\%$) and it decreases towards the sidewall surfaces at the rate of about $0.4\%/\mu$m.

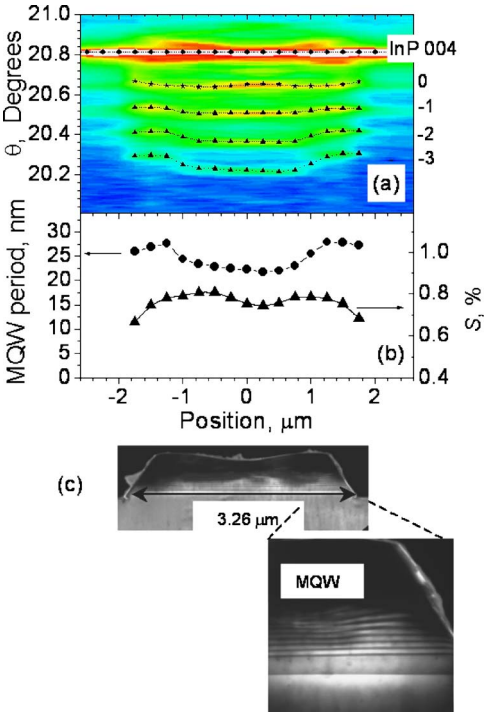

FIG. 3. (Color online) Cross-section analysis of the InGaAsP-based MQW SAG structure. (a), (b), and (c) are the same as in Fig. 2. The TEM inset magnifies the sidewall part of the structure.

The InGaAsP-based sample, however, demonstrates a significant variation of the MQW period across the ridge from 22.1 nm in the center to 27.8 nm at the edges (Fig. 3). These data agree with the TEM image [Fig. 3(c)], where both the overgrowth in the InP cap layer and the increase of the period can be seen. Additional growth enhancement at the sidewalls of the ridge is well known for phosphorus-based SAG structures, and is usually explained by insufficient surface migration of group-III precursors during growth.[2,3] We found that the global MQW strain increases at the position of the overgrowth peaks ($S=0.80\%$) compared to the lower value in the center of the ridge ($S=0.75\%$), indicating compositional changes as well. Since the group-V element composition (As/P) ratio is constant in the SAG growth across the entire wafer (see Refs. 2 and 3), then the strain increase should correspond to changes in the group-III ratio. Thus, the enhanced incorporation of indium, which is affected more strongly by the insufficient surface migration, can explain the additional strain and a thickness increase in the overgrown regions. The obvious difference compared to Al-based sample is the presence of phosphorus in the InGaAsP-based MQW structure. During growth, the strong In–P bonding results in the accumulation of indium on the 001 plane close to the sidewalls of the waveguides. Assuming equal contributions of the surface migration effects to the composition change of the wells and barriers in our MQW structure, we estimate that the average indium composition increase between the center and the overgrown part of the ridge is 0.6%. Closer to the sidewalls of the ridge, the global MQW strain relaxes from $S=0.80\%$ at the overgrowth peaks to $S=0.65\%$ with a strain gradient of about $0.3\%/\mu$m, a value which is close to that in the Al-based SAG structure, though the average strain variation across the entire ridge is less than in Al-based structure. This result demonstrates that the excessive incorporation of indium due to insufficient surface migration can increase the strain at the vicinity of the sidewalls, thus competing with the strain relaxation at the free-standing surface of the ridges.

In conclusion, we found that cross-section thickness uniformity of the Al-based SAG MQWs is superior compared to that of traditional P-based structures, which is promising for development of a one-growth-step technology for uncooled high-density integrated optoelectronic devices. Strain relaxation at the sidewalls of the P-based waveguides is suppressed by excessive incorporation of indium, which can be important for strain manipulation in the regime of nanoepitaxy of lattice-mismatched materials.

The authors thank K. Bacher, L. J. P. Ketelsen, and W. Hobson for their support and interest in these studies. Use of the Advances Photon Source was supported by the U.S. Department of Energy, Office of Science, Office of Basic Energy Sciences, under Contract No. W-31-109-ENG-38. The Cornell High Energy Synchrotron Source was supported by the National Science Foundation and the National Institutes of Health/National Institute of General Medical Sciences under Award DMR-0225180.

[1]N. N. Ledentsov and D. Bimberg, J. Cryst. Growth **255**, 68 (2003).
[2]T. Van Caenegem, I. Moerman, and P. Demeester, Prog. Cryst. Growth Charact. Mater. **35**, 263 (1997).
[3]M. Gibbon, J. P. Stagg, C. G. Cureton, E. J. Thrush, C. J. Jones, R. E. Mallard, R. E. Pritchard, N. Collis, and A. Chew, Semicond. Sci. Technol. **8**, 998 (1993).
[4]M. A. Alam, R. People, E. D. Isaacs, K. Evans-Lutterodt, T. Siegrist, T. Pernell, J. Vandenberg, S. K. Sputz, S. N. G. Chu, D. V. Lang, L. Smith, and M. Hybertsen, Appl. Phys. Lett. **74**, 2617 (1999).
[5]A. A. Sirenko, A. Kazimirov, R. Huang, D. H. Bilderback, S. O'Malley, V. Gupta, K. Bacher, L. J. P. Ketelsen, and A. Ougazzaden, J. Appl. Phys. **97**, 063512 (2005).
[6]Z. Cai, B. Lai, and S. Xu, J. Phys. IV **104**, 17 (2003).
[7]M. Wormington, C. Panaccione, K. M. Matney, and K. D. Bowen, Philos. Trans. R. Soc. London, Ser. A **357**, 2827 (1999).
[8]Z.-H. Cai, W. Rodrigues, P. Ilinski, D. Legnini, B. Lai, W. Yun, E. D. Isaacs, K. E. Lutterodt, J. Grenko, R. Glew, S. Sputz, J. Vandenberg, R. People, M. A. Alam, M. Hybertsen, and L. J. P. Ketelsen, Appl. Phys. Lett. **75**, 100 (1999).
[9]S. Kimura, H. Kimura, K. Kobayashi, T. Oohira, K. Izumi, Y. Sakata, Y. Tsusaka, K. Yokoyama, S. Takeda, M. Urakawa, Y. Kagoshima, and J. Matsui, Appl. Phys. Lett. **77**, 1286 (2000).
[10]A. Kazimirov, D. H. Bilderback, R. Huang, and A. Sirenko, AIP Proceedings 705, edited by J. Stohr, H. A. Padmore, T. Warwick, and J. Arthur (AIP, New York, 2004), p. 1027.
[11]A. Kazimirov, D. H. Bilderback, R. Huang, A. Sirenko, A. Ougazzaden, J. Phys. D **37**, L9 (2004).
[12]T. Fujii and M. Ekawa, J. Appl. Phys. **78**, 5373 (1995).
[13]J. E. Greenspan, X. Zhang, N. Puetz, and B. Emmerstorfer, J. Vac. Sci. Technol. A **18**, 648 (2000).
[14]Y. Sakata, Y. Inomoto, and K. Komatsu, J. Cryst. Growth **208**, 130 (2000).
[15]S. Kimura, Y. Kagoshima, T. Koyama, I. Wada, T. Niimi, Y. Tsusaka, J. Matsui, and K. Izumi, in Ref. 10.
[16]L. Tapfer, G. C. La Rocca, H. Lage, O. Brandt, D. Heitmann, and K. Ploog, Appl. Surf. Sci. **60/61**, 517 (1992).
[17]For MOVPE growth controlled by diffusion, the uniform thickness across a certain area of the wafer corresponds to a constant growth rate, which can be explained only by a uniform composition in such area. Otherwise (composition changes across the ridge, but thickness is uniform), in the diffusion model describing such an improbable situation, at least one of the precursors should migrate along the gradient of its own concentration.